ACS APPLIED NANO MATERIALS

www.acsanm.org Article

Quantum Dots Electrostatically Adsorbed on the Surface of SiO_2 Nanoparticle-Decorated Phosphor Particles for White Light-Emitting Diodes with a Stable Optical Performance

Shuling Zhou, Xuan Yang, Xingjian Yu, Bin Xie, Xinfeng Zhang, Wei Lan, Zhaojin Wang, Kai Wang,* and Xiaobing Luo*

Cite This: *ACS Appl. Nano Mater.* 2020, 3, 12394−12400 Read Online

ACCESS | Metrics & More | Article Recommendations | Supporting Information

ABSTRACT: White light-emitting diodes (WLEDs) based on phosphor and quantum dots (QDs) have attracted worldwide attention. Phosphor and QDs with different physical characteristics are distributed unevenly in a polymer matrix, resulting in the spectrum changes of the phosphor-QD-based WLEDs (PQ-WLEDs). Aiming for a similar distribution of QDs and phosphor in the matrix, we proposed the phosphor/SiO_2/QD (PSQ) composite particles in which negatively charged QDs are electrostatically adsorbed on the surface of phosphor particles decorated with positively charged SiO_2. The PSQ composite particles retained a high quantum yield of 77.6%. PSQ-WLEDs with varied standing times of the uncured PSQ-added silicone showed stable spectra with stable optical parameters. For comparison, the spectra of PQ-WLEDs with untreated phosphor and QDs obviously changed with the standing time. Specifically, the LE, CCT, and CRI of PSQ-WLEDs using Dow corning OE 180 silicone only changed by 1.7, 3.3, and 3.9%, respectively, after a long sufficient standing time; however, the LE, CCT, and CRI of PQ-WLEDs using the same silicone changed by 9, 5.4, and 10%, respectively. This optical instability in PQ-WLEDs resulted from the difference between the distribution of phosphor and QDs in the mixed silicone matrix after standing. However, the distribution of phosphor and QDs in PSQ-WLEDs was always the same with each other due to the composite structure. Applying the PSQ composite particles in WLEDs, we can easily attain highly optical consistent phosphor-QD-based WLEDs and provide an efficient control of product quality.

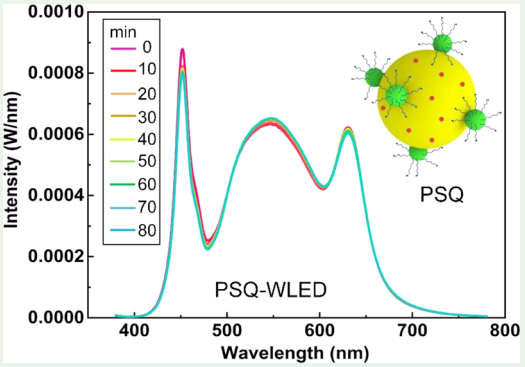

KEYWORDS: *composites, quantum dots, phosphor, light-emitting diodes, sedimentation, optical consistency*

1. INTRODUCTION

Common white light-emitting diodes (WLEDs) containing blue light-emitting chips and yellow light-emitting phosphor have high luminous efficiencies (LEs) but low color rendering indexes (CRIs) because of the lack of red light.[1,2] Quantum dots (QDs) as luminescent nano-semiconductor materials have shown excellent advantages in wavelength turnability and color rendering capability in the application of WLEDs.[3−7] A phosphor and QDs-converted WLED (PQ-WLED) can achieve high LE and CRI, simultaneously.[7−10] During the packaging of PQ-WLEDs, QDs and phosphor are uniformly mixed in a polymer such as silicone with a certain viscosity and behave differently: phosphor with a diameter of several microns undergoes sinking in the viscous silicone,[11,12] but the nanometer-sized QDs stay in suspension. After several minutes, phosphor is distributed in a gradient concentration in silicone but QDs are still distributed uniformly. The different distributions of phosphor and QDs change their light-emitting intensity because phosphor situated at the bottom gets more exciting blue light than the QDs.[13−15]

Many researchers have studied the effects of changeable distribution of phosphor in silicone on the spectra and optical parameters of phosphor-converted WLEDs.[16,17] Avoiding phosphor sinking is a direct way to maintain the stable distribution of phosphor. Researchers have provided some methods to evenly distribute phosphor in silicone of WLEDs, such as the modified phosphor with vinylsilane coupling agent,[18] phosphor/silicone particles,[19] and phosphor/glass.[20,21] However, these methods are unsuitable for the phosphor and QDs-added WLEDs for the following reasons: the high manufacturing temperature of phosphor/glass will thermally quench the QDs, and the phosphor/silicone and modified

Received: November 5, 2020
Accepted: November 23, 2020
Published: December 2, 2020

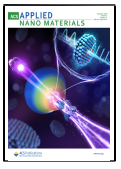

https://dx.doi.org/10.1021/acsanm.0c02947
ACS Appl. Nano Mater. 2020, 3, 12394−12400

phosphor just slow down the sinking of phosphor instead of avoiding.

We proposed a new idea to maintain the distribution of QDs similar to that of phosphor in silicone of WLEDs by producing the phosphor/SiO_2/QD (PSQ) composite particles. The PSQ composite synthesized by electrostatic adsorption is a whole new approach to avoid uneven distribution of phosphor and QDs, which is responsible for the different spectra and optical characteristics of WLEDs. The PSQ particles will sink as the pure phosphor does, and the QDs will have the same distribution with phosphor to catch the same blue light in different sinking conditions. Phosphor is much harder to be positively charged by a reaction with amino-terminal silicane than SiO_2. Therefore, SiO_2 was generated on the surface of phosphor, following a facile amino-modification, which positively charged the SiO_2-coated phosphor. Then, the electropositive phosphor/SiO_2 (PS) combined with the electronegative carboxyl-terminal QDs. Figure 1a shows the schematic of the PSQ composite particles. SiO_2 spheres are located on the surface of phosphor and QDs on the surface of the composite phosphor/SiO_2 (PS).

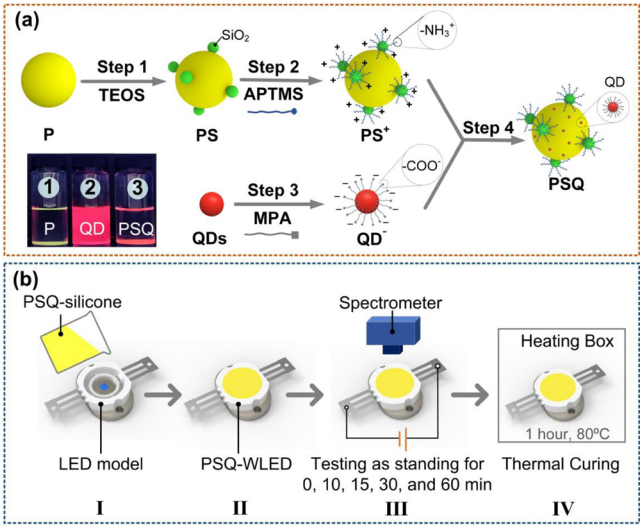

Figure 1. Schematic of (a) the manufacture of the PSQ composite particles and (b) process of PSQ-WLED packaging and optical measurement.

2. EXPERIMENTAL SECTION

According to the manufacturing process shown in Figure 1a, we prepared the PSQ composite particles in four steps. The first step was to generate the SiO_2-coated phosphor (PS) by hydrolyzing tetraethylorthosilicate (TEOS) via a sol–gel method:[22] 1 g of phosphor (the yellow-greenish YAG:Ce phosphor with a peak wavelength of 550 nm), 20 mL of ethanol, 5 mL of deionized water, and 1 mL of TEOS were mixed. Then, 1 mL of ammonium hydroxide was added dropwise into the mixture and stirred for 30 min at 60 °C; the attained PS precipitation was washed twice by ethanol. The second and third steps followed a previously described method.[23] The second step was to modify the PS with amino ions from 3-aminopropyl trimethoxysilane (APTMS): a mixture of 1 g of phosphor/SiO_2, 20 mL of ethanol, and 5 mL of APTMS were stirred for 7 h at 25 °C; the generated PS^+ precipitation was washed twice by ethanol and kept in 10 mL of deionized water. The third step was to modify the QDs with carboxyl anions from 3-mercaptopropionic (MPA): 2 mL of MPA, 6 mL of sodium hydroxide solution (1 g of NaOH in 10 mL of water), and 10 mg of QDs (red-emissive CdSe/CdS core/shell QDs with oleic acid ligands and a peak wavelength of 630 nm) in 3 mL of chloroform were mixed and stirred for 10 min; this mixture was extracted by 5 mL of deionized water and centrifuged; the generated QD^- precipitation was dispersed in 5 mL of deionized water. The final step was the electrostatic combination: 1 mL of the carboxyl-anion-terminal QD^- solution (containing 2 mg of QDs) was added dropwise in 10 mL of stirred amino-ion-terminal PS^+ solution (containing 1 g of phosphor). The final orange precipitate, the PSQ composite particles, was dried for 12 h at 50 °C. In the lower left of Figure 1a, the prepared PSQ particles in Bottle 3 can entirely sink like pure phosphor (P) in Bottle 1, and the QDs evenly suspend in chloroform in Bottle 2.

Figure 1b illustrates the process of PSQ-WLED packaging and optical measurement. The InGaN chips (peak wavelength of 450 nm) in the LED model were covered with 0.1 g of 10 wt % PSQ-added silicone resin. Two kinds of silicone resins with different viscosities were used (Dow corning OE 184 with a viscosity of 3500 cP, Dow corning OE 6550 with a viscosity of 4700 cP). The spectra of PSQ-WLED with uncured silicone mixture were tested after standing for 0, 10, 15, 30, and 60 min at room temperature of 25 °C. The applied Dow corning OE silicone needs at least 12 h to cure thoroughly at room temperature. Main optical parameters, such as CCT, LE, CRI, and chromaticity coordinates, were calculated from the obtained spectra. After the optical test, the composite silicone of the PSQ-WLED was cured at 80 °C for 1 h. For comparison, a PQ-WLED added with pure phosphor and QDs was packaged and tested. For a fair comparison of luminous efficiency, CCT and CRI of PQ-WLED were adjusted to be similar to those of PSQ-WLED.

Scanning electron microscopy (SEM) images were measured by an FEI Nova NanoSEM 450. Transmission electron microscopy (TEM) images were measured by a Tecnai G2 F30 transmission electron microscope. Fourier transform infrared spectroscopy (FTIR) images were measured by a Thermo Nicolet iS50. Surface charges of QD^- and PS^+ particles were measured using a Zeta-Potential Analyzer (Brookhaven BI-200SM). The cross-sectional pictures of PSQ (phosphor and QDs)-added silicone films were taken by a photon microscope. The photoluminescence (PL) spectra and absolute PL quantum yields were measured by a Hamamatsu Quantaurus-QY at an excitation wavelength of 450 nm from a xenon lamp. Time-resolved PL (TRPL) spectra were measured by an FLS 980 Series of Fluorescence Spectrometer at a pulse excitation wavelength of 450 nm. The spectra of the PQ-WLED and the PSQ-WLED were tested by an Everfine ATA-1000 Integrating Sphere at 100 mA of current.

3. RESULTS AND DISCUSSION

3.1. Morphology. Figure 2 shows a series of SEM and TEM images to visually observe the materials and products during the preparation of PSQ. The sphere-like phosphor (P) in Figure 2a,b has a diameter of about 10 μm and a smooth surface. In Figure 2c,d, the PS particles were coated with many small SiO_2 particles. The nanoscale QDs with a uniform size are shown in Figure 2e,f. The SiO_2 particles and synthesized SiO_2/QDs (SQ) are shown in Figure 2g,h, respectively, proving the electrostatic adsorption between the amino-terminal SiO_2 and carboxyl-terminal QDs. A single PSQ particle and its partially enlarged details are shown in Figure 2i–k, respectively. In the PSQ particle, SiO_2 particles were coated on the surface of phosphor and QDs on the surfaces of SiO_2 and phosphor.

Figure 3a,b shows the FTIR spectra of the above-mentioned materials and products. In Figure 3a, due to the wide absorbance wavenumber range of phosphor, its FTIR spectra show a fake "negative" peak around 1000 cm^{-1} of wavenumber. The real positive absorbance peak of the Si–O bond appeared at 1115 cm^{-1} (point A) in the FTIR spectra of (PS) phosphor/SiO_2 due to the coating of SiO_2. The PS^+ (PS/APTMS) had a weak absorption peak at 2939 cm^{-1} (point B, the C–H bond

https://dx.doi.org/10.1021/acsanm.0c02947
ACS Appl. Nano Mater. 2020, 3, 12394–12400

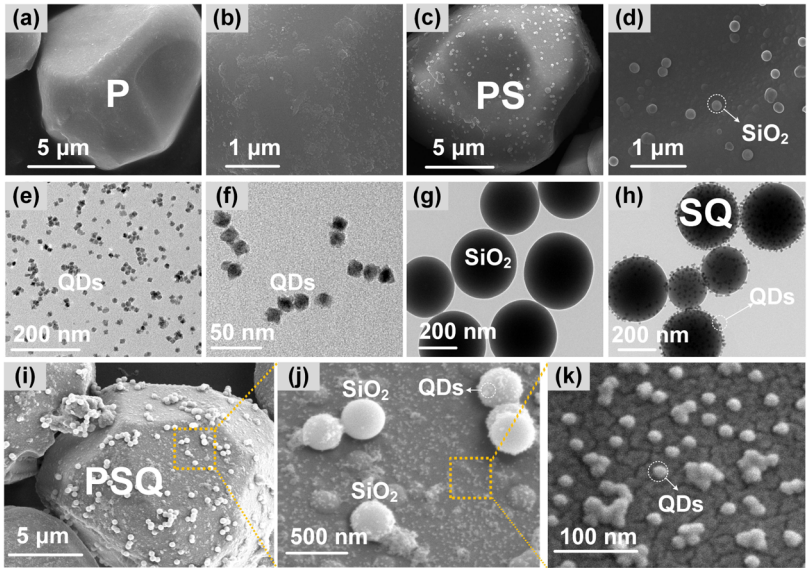

Figure 2. SEM images of (a, b) phosphor, (c, d) PS, and (i, j, k) PSQ. TEM images of (e, f) QDs, (g) SiO_2, and (h) SQ.

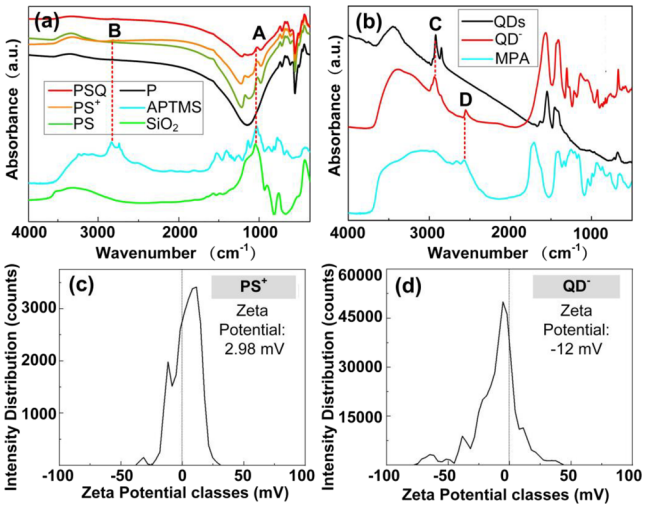

Figure 3. (a) FTIR spectra of phosphor (P), SiO_2, PS, APTMS, PS^+, and PSQ; (b) FTIR spectra of QDs, MPA, and QD^-; (c) charge potential of PS^+; and (d) charge potential of QD^-.

in CH_2) from the reaction with a small amount of APTMS. The absorbance spectrum of PSQ hardly shows a peak of QDs due to the very little coating of QDs. In Figure 3b, the absorbance spectrum of QDs shows some obvious peaks from the oleic acid ligand, such as the peaks at 3448 cm^{-1} (the O−H bond) and 1575 cm^{-1} (the C═O bond). The absorbance spectrum of the QD^- (QDs/MPA) was not only similar to that of the MPA but also had a same peak (the C−H bond in CH_2) with QDs at 2921 cm^{-1} (point C) and another same peak (the S−H bond) with MPA at 2552 cm^{-1} (point D). The existence of the above bonds proved the accuracy of the products during the synthesis process of PSQ displayed in Figure 1a. As shown in Figure 3c,d, zeta-potential test results show that the charge potentials of PS^+ and QD^- were +2.98 and −12 mV, respectively. The opposite charge potentials of modified phosphor and QDs strongly confirmed the fabrication principle of PSQ by electric absorption.

The cross sections of PSQ-added silicone films and phosphor and QD (P + Q)-added silicone films are shown in Figure 4a,b, respectively. All of the films were cured at 80 °C for 1 h after 0 or 60 min of standing at room temperature of 25

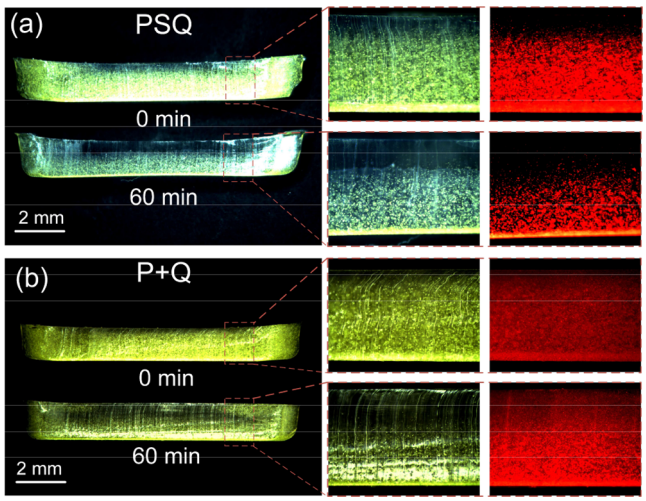

Figure 4. Microscopic photos of the cross sections of (a) PSQ-silicone films and (b) P + Q-silicone films after 0 and 60 min of standing times, respectively.

°C. PSQ and P obviously sank in silicone films after 60 min of standing. However, the upper layer of the PSQ-silicone film under ultraviolet light was blank signifying the absence of luminescent particles here, which was different from the still light-emitting upper layer of the P + Q-silicone film. QDs in PSQ-silicone films moved with phosphor and shared the same distribution of phosphor due to their combination, but QDs in P + Q-silicone films were always suspended leading the upper layer with only QDs after the sinking of phosphor and the different distributions between QDs and phosphor.

3.2. Effects of Modifications and Optical Performance of PSQ. Photoluminescence (PL) spectra of pure and modified phosphor and QDs are shown in Figure 5a. As for phosphor, the PL spectra of pure phosphor, PS, and PS^+ were almost the same and their quantum yields (QYs) were 0.977, 0.991, and 0.996, respectively. Coating and modifying hardly

https://dx.doi.org/10.1021/acsanm.0c02947
ACS Appl. Nano Mater. 2020, 3, 12394−12400

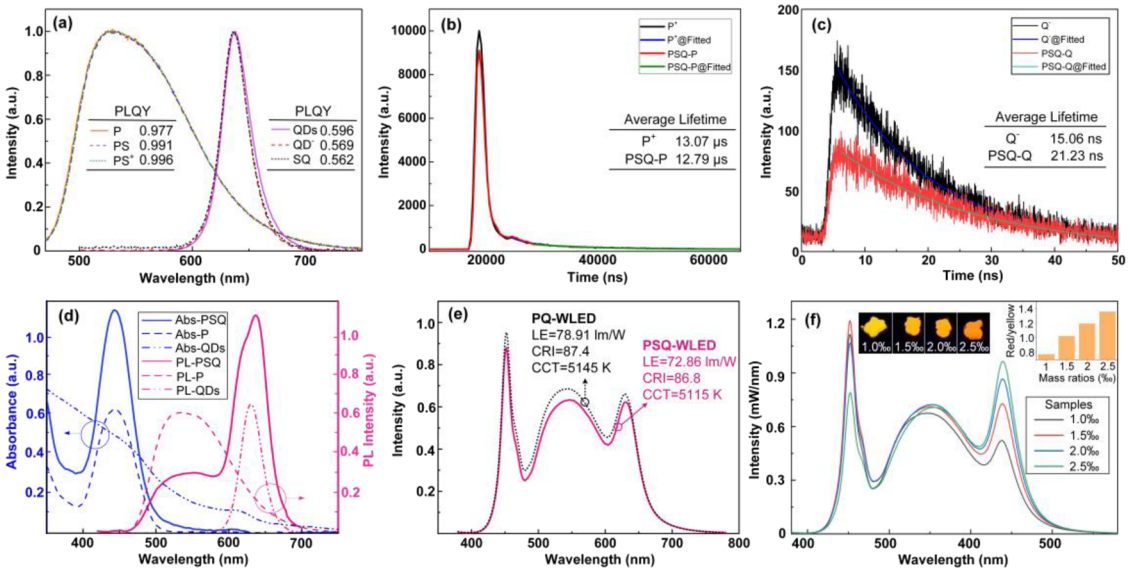

Figure 5. (a) PL spectra of the pure and modified phosphor and QDs; (b) TRPL spectra of positively charged phosphor and phosphor in PSQ; (c) TRPL spectra of negatively charged QDs and QDs in PSQ; (d) absorbance and emission spectra of PSQ, phosphor, and QDs; (e) normalized spectra of PQ-WLED and PSQ-WLED; and (f) spectra of PSQ-WLED with different-colored PSQ.

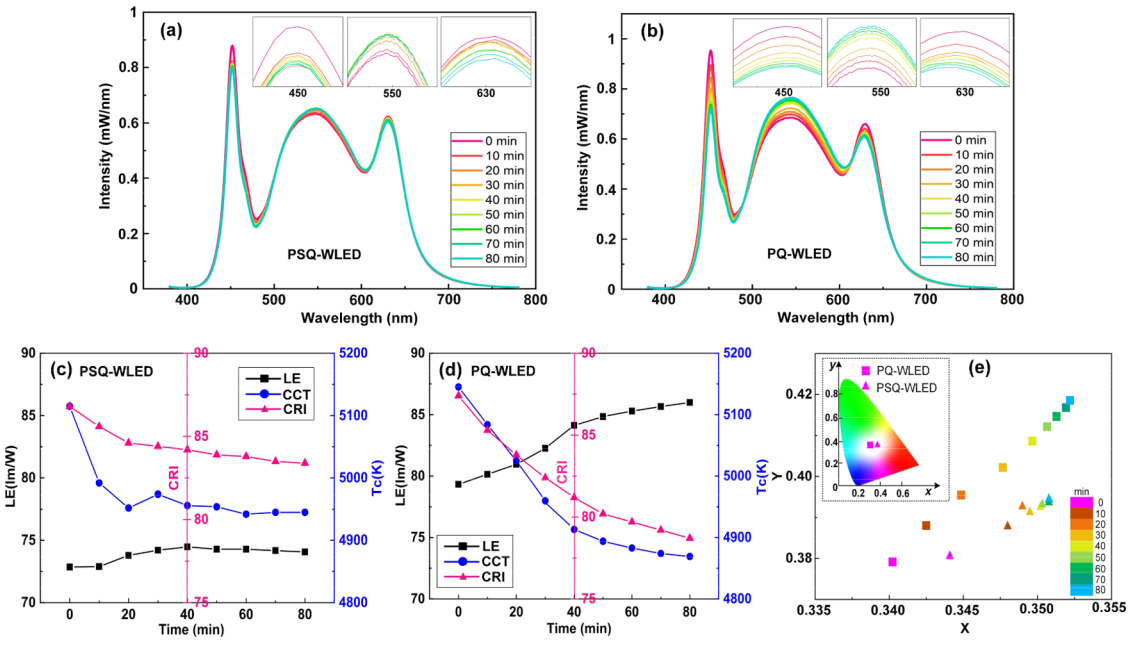

Figure 6. Spectra of (a) PSQ-WLED and (b) PQ-WLED after different standing times; variations of LE, CCT, and CRI of (c) PSQ-WLED and (d) PQ-WLED; and (e) comparison of their CIE coordinates.

affected the optical transfer ability of phosphor because of the negligible small coverage rate of SiO_2 particles. As for QDs, compared with pure QDs with a QY of 0.596, the PL spectra of QD^- and SQ slightly shifted to red, and their QYs reduced to 0.569 by 4.5% and 0.562 by 5.7%, respectively. The surface defects resulting from the ligand exchange during the MPA modification of QDs and the light optical absorption of SiO_2 would reduce the QY of modified QDs.

Fluorescence decay curves of phosphor (QDs) in both P^+ (QD^-) and PSQ are shown in Figure 5b,c. These decay curves were well fitted with an exponential function $I(t) = A\,e^{-t/\tau}$, where $I(t)$ is the PL intensity at time t and τ is the PL lifetime. It has been noted that the fluorescence decay of PSQ was measured at both microsecond and nanosecond levels because the PL lifetimes of YAG phosphor and CdSe/CdS QDs in PSQ were several microseconds and nanoseconds, respectively. Phosphor in PSQ (12.79 μs) had a shorter PL lifetime than that of P^+ (13.07 μs) by 2%, but QDs in PSQ (21.23 ns) had a much longer PL lifetime than that of QD^- (15.06 ns) by 41%. The PL lifetime changes of phosphor and QDs in PSQ were caused by the fluorescence resonance energy transfer from phosphor to the attached QDs.[24,25]

Absorbance and emission spectra of PSQ composite particles, phosphor, and QDs are shown in Figure 5d. The absorbance spectrum of QDs had a wide range of absorption wavelength, different from the obvious absorbance peak of phosphor at 445 nm. The absorbance spectrum of PSQ was similar to that of phosphor with an absorption peak. There

https://dx.doi.org/10.1021/acsanm.0c02947
ACS Appl. Nano Mater. 2020, 3, 12394−12400

were two peak wavelengths in the emission spectra of PSQ at 550 and 630 nm, inheriting from phosphor and QDs, respectively. In addition, the QY of PSQ was 77.6% under an exciting wavelength of 450 nm.

Normalization spectra of the PSQ-WLED and PQ-WLED are compared in Figure 5e. As mentioned before, both kinds of WLEDs possessed similar CCT and CRT for a fair comparison of LE. The CCT, CRI, and LE of PSQ-WLED were 5115 K, 86.8, and 72.86 lm/W, respectively, and those of PQ-WLED were 5145 K, 87.4, and 78.91 lm/W, respectively. The LE of PSQ-WLED was 7.6% less than that of PQ-WLED due to several reasons for light loss, such as the slight reduction of the QY of QDs after modification and the fluorescence resonance energy transfer from phosphor to the attached QDs, which was proved above by the PL lifetime changes of phosphor and QDs in PSQ.

The color of PSQ particles was adjustable by changing the mass ratios of QDs in PSQ. As shown in Figure 5f, PSQ of four mass ratios (1.0, 1.5, 2.0, and 2.5‰) was synthesized, and their colors gradually turned from yellow to orange with the increase of QDs. The intensities of red-emitting light in the spectra of PSQ-WLED were also enhanced with larger mass ratios of QDs in PSQ. This color turnability of PSQ can be applied to package PSQ-WLED of varied CCT or CIR.

3.3. Optical Stability of PSQ-WLEDs. Figure 6a shows the stable spectra of the PSQ-WLED after standing for several minutes. However, the spectra of the PQ-WLED changed with the standing time of phosphor and QDs-mixed silicone, yellow light enhanced while blue light and red light reduced, as shown in Figure 6b. Variations in LE, CCT, and CRI of PSQ-WLED were obviously smaller than those of PQ-WLED. After standing for 80 min, as shown in Figure 6c, LE of PSQ-WLED increased only by 1.7%, and its CCT and CRI reduced by 3.3 and 3.9%, respectively; but, as shown in Figure 6d, LE of PQ-WLED increased obviously by 9%, and its CCT and CRI reduced sharply by 5.4 and 10%, respectively. In addition, Figure 6e shows that the CIE coordinates of the PSQ-WLED moved slowly from $x = 0.344$ and $y = 0.380$ to $x = 0.350$ and $y = 0.394$ with increasing the standing time from 0 to 80 min, but the CIE coordinates of the PQ-WLED moved sharply from $x = 0.340$ and $y = 0.379$ to $x = 0.352$ and $y = 0.418$. From the view of efficiency, the PSQ-WLED spent less time to achieve the stability of spectra. Slight changes in the optical characteristics of the PSQ-WLED were acceptable. It has been noted that the viscosity of silicone affects the sinking speed of phosphor in mixed silicone. WLEDs in Figure 6 used the Dow corning OE 180 with a viscosity of 3500 cP. Another kind of silicone with a larger viscosity (Dow corning OE 6550, viscosity of 4700 cP) was also used to package PSQ-WLED and PQ-WLED. The optical parameter variations are shown in Table 1. Even though larger viscosity of silicone can slow down the sinking of phosphor, the spectra of PQ-WLED with Dow corning OE 6550 silicone still changed much more than that of PSQ-WLED with the same silicone after standing, as shown in Figure S1. In a word, PSQ-WLED with PSQ composite particles displayed a much more stable optical performance than PQ-WLED with pure phosphor and QDs.

Table 1. Optical Parameter Changes in PSQ-WLED and PQ-WLED with Different Silicone Films

silicone	WLED	LE (%)	CCT (%)	CRI (%)
Dow corning OE 180	PSQ	1.7	3.3	3.9
	PQ	9	5.4	10
Dow corning OE 6550	PSQ	5.8	0.1	0.3
	PQ	14.2	11.8	5.7

The sinking of luminescent particles influences the optical performances of PQ-WLED and PSQ-WLED in different ways, as shown in Figure 7. As for PQ-WLED, on the one hand,

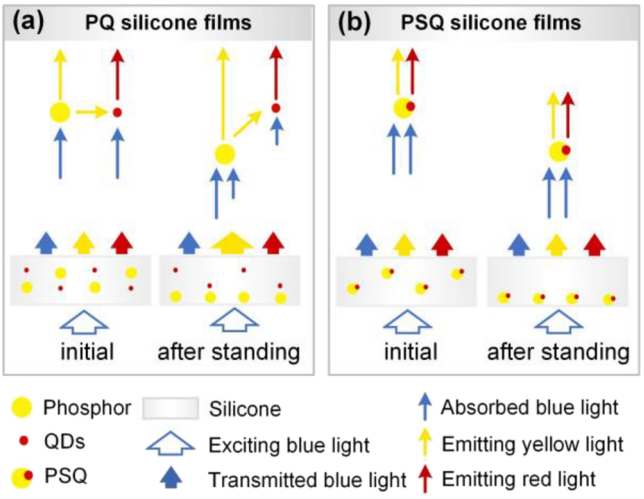

Figure 7. Schematic of the optical performance of (a) the PQ silicone films and (b) the PSQ-silicone films in the initial and after standing.

phosphor gathered in the lower part of the silicone film (close to the chip) after standing and caught more blue light than QDs, so that the emission intensity of yellow light from phosphor increased; on the other hand, QDs caught less blue light but more yellow light due to the wide absorption spectrum from the ultraviolet to the visible light. The longer the PQ-WLED was left standing, the higher the intensity of yellow-emitting light from phosphor and the lower the intensity of red-emitting light from QDs. As for PSQ-WLED, though the PSQ composite particles also sank and gathered in the lower part of the silicone layer, phosphor and QDs always caught the blue light at the same time because their distances from chips were always the same no matter how the PSQ was distributed. Therefore, the essence of achieving optical stability by PSQ-WLEDs with different standing times was in the similar distribution of phosphor and QDs due to their connection.

4. CONCLUSIONS

The graded-distributed phosphor and uniform-distributed QDs in the silicone matrix led to spectrum changes in the phosphor-QD-based WLEDs. Therefore, we provided PSQ composite particles to enable the even distribution of phosphor and QDs in the silicone matrix. The synthesized PSQ possessed a high QY of 77.6%. Besides, the emitting spectrum of the PSQ particles was alterable by controlling the mass ratios of ingredients. A PSQ-WLED with PSQ and a PQ-WLED with pure phosphor and QDs were fabricated and tested. The PSQ-WLED showed more stable spectra and higher optical consistency after varied standing times than those of the PQ-WLED. For example, the LE, CCT, and CRI of PSQ-WLED using Dow corning OE 180 silicone changed only by 1.7, 3.3, and 3.9%, respectively, after a long sufficient standing time; however, the LE, CCT, and CRI of PQ-WLED

https://dx.doi.org/10.1021/acsanm.0c02947
ACS Appl. Nano Mater. 2020, 3, 12394−12400

using the same silicone changed by 9, 5.4, and 10%, respectively. It is good to note that by the application of PSQ in WLEDs, we can achieve phosphor and QD-based WLEDs of higher optical consistency. No matter how the distribution of PSQ changes, the spectrum of the PSQ-WLED was highly stable. In other words, we can apply the PSQ particles to easily attain a highly optical consistent phosphor-QDs-based WLED regardless of many factors affecting the particles' distribution in the packaging polymer, which provides an efficient control and management of product quality.

■ ASSOCIATED CONTENT

Supporting Information

The Supporting Information is available free of charge at https://pubs.acs.org/doi/10.1021/acsanm.0c02947.

Spectra of PSQ-WLED (PQ-WLED) using the Dow corning OE 6550 silicone for matrix of PSQ (phosphor and QDs) after different standing time; variations of LE, CCT, and CRI of PSQ-WLED and PQ-WLED; and CIE coordinates shifts of PSQ-WLED and PQ-WLED (PDF)

■ AUTHOR INFORMATION

Corresponding Authors

Kai Wang − *Department of Electrical and Electronic Engineering, Southern University of Science and Technology, Shenzhen 518055, China;* orcid.org/0000-0003-0443-6955; Email: wangk@sustc.edu.cn

Xiaobing Luo − *State Key Laboratory of Combustion, School of Energy and Power Engineering, Huazhong University of Science and Technology, Wuhan 430074, China; Wuhan National Laboratory for Optoelectronics, Wuhan 430074, China;* orcid.org/0000-0002-6423-9868; Email: luoxb@hust.edu.cn

Authors

Shuling Zhou − *State Key Laboratory of Combustion, School of Energy and Power Engineering, Huazhong University of Science and Technology, Wuhan 430074, China*

Xuan Yang − *State Key Laboratory of Combustion, School of Energy and Power Engineering, Huazhong University of Science and Technology, Wuhan 430074, China*

Xingjian Yu − *State Key Laboratory of Combustion, School of Energy and Power Engineering, Huazhong University of Science and Technology, Wuhan 430074, China*

Bin Xie − *State Key Laboratory of Combustion, School of Energy and Power Engineering, Huazhong University of Science and Technology, Wuhan 430074, China*

Xinfeng Zhang − *State Key Laboratory of Combustion, School of Energy and Power Engineering, Huazhong University of Science and Technology, Wuhan 430074, China*

Wei Lan − *State Key Laboratory of Combustion, School of Energy and Power Engineering, Huazhong University of Science and Technology, Wuhan 430074, China*

Zhaojin Wang − *Department of Electrical and Electronic Engineering, Southern University of Science and Technology, Shenzhen 518055, China*

Complete contact information is available at: https://pubs.acs.org/10.1021/acsanm.0c02947

Notes

The authors declare no competing financial interest.

■ ACKNOWLEDGMENTS

This work was supported by the National Natural Science Foundation of China (51625601), the Ministry of Science and Technology of the People's Republic of China (2017YFE0100600), the Creative Research Groups Funding of Hubei Province (2018CFA001), the Open Project Program of Wuhan National Laboratory for Optoelectronics (2018WNLOKF017), the Natural Science Foundation of Guangdong (2017B030306010), and the China Postdoctoral Science Foundation (2020M672346).

■ REFERENCES

(1) Shur, M. S.; Žukauskas, A. Solid-State Lighting: Toward Superior Illumination. *Proc. IEEE* **2005**, *93*, 1691−1703.

(2) Pimputkar, S.; Speck, J. S.; Denbaars, S. P.; Nakamura, S. Prospects for LED lighting. *Nat. Photonics* **2009**, *3*, 180−182.

(3) Anikeeva, P. O.; Halpert, E. J.; Bawendi, G. M.; Bulović, V. Quantum Dot Light-Emitting Devices with Electroluminescence Tunable over the Entire Visible Spectrum. *Nano Lett.* **2009**, *9*, 2532−2536.

(4) Chen, O.; Zhao, J.; Chauhan, V. P.; Cui, J.; Wong, C.; Harris, D. K.; Wei, H.; Han, H.-S.; Fukumura, D.; Jain, R. K.; Bawendi, M. G. Compact high-quality CdSe/CdS Core/shell Nanocrystals with Narrow Emission Linewidths and Suppressed Blinking. *Nat. Mater.* **2013**, *12*, 445−451.

(5) Kagan, C. R.; Lifshitz, E.; Sargent, E. H.; Talapin, D. V. Building Devices from Colloidal Quantum Dots. *Science* **2016**, *353*, No. aac5523.

(6) Wang, Y.; Zheng, J.; Wang, J.; Yang, Y.; Liu, X. Rapid Microwave-assisted Synthesis of Highly Luminescent Nitrogen-doped Carbon Dots for White Light-emitting Diodes. *Opt. Mater.* **2017**, *73*, 319−329.

(7) Li, J.; Tang, Y.; Li, Z.; Ding, X.; Yu, B.; Lin, L. Largely Enhancing Luminous Efficacy, Color-Conversion Efficiency, and Stability for Quantum-Dot White LEDs Using the Two-Dimensional Hexagonal Pore Structure of SBA-15 Mesoporous Particles. *ACS Appl. Mater. Interfaces* **2019**, *11*, 18808−18816.

(8) Xie, B.; Hu, R.; Luo, X. Quantum Dots-converted Light-emitting Diodes Packaging for Lighting and Display: Status and Perspectives. *J. Electron. Packag.* **2016**, *138*, No. 020803.

(9) Ding, Y.; Zheng, J.; Wang, J.; Yang, Y.; Liu, X. Direct Blending of Multicolor Carbon Quantum dots into Fluorescent Films for White Light Emitting Diodes with an Adjustable Correlated Color Temperature. *J. Mater. Chem. C* **2019**, *7*, 1502−1509.

(10) Yin, L.; Hu, Y.; Yang, Z.; Zhou, J.; Li, W.; Zhang, Y. Silicon-coated CdZnSeS/ZnS Quantum Dots Contribute to Great Performance White Light-emitting Diodes. *J. Lumin.* **2020**, *220*, No. 116969.

(11) Wang, Y.; Zheng, H.; Hu, R.; Luo, X. Modeling on Phosphor Sedimentation Phenomenon during Curing Process of High Power LED Packaging. *J. Solid State Light.* **2014**, *1*, No. 2.

(12) Yang, T.-H.; Chen, C.-C.; Chen, C.-Y.; Chang, Y.-Y.; Sun, C.-C. Essential Factor for Determining Optical Output of Phosphor-converted LEDs. *IEEE Photonics J.* **2014**, *6*, No. 8200209.

(13) Xie, B.; Chen, W.; Hao, J.; Wu, D.; Yu, X.; Cheng, Y.; Hu, R.; Wang, K.; Luo, X. Structural Optimization for Remote White Light-emitting Diodes with Quantum Dots and Phosphor: Packaging Sequence Matters. *Opt. Express* **2016**, *24*, A1560−A1570.

(14) Tang, Y.; Lu, H.; Li, J.; Li, Z.; Du, X.; Ding, X.; Yu, B. Improvement of Optical and Thermal Properties for Quantum Dots WLEDs by Controlling Layer Location. *IEEE Access* **2019**, *7*, 77642−77648.

(15) Li, Z.; Zheng, J.; Li, J.; Zhan, W.; Tang, Y. Efficiency Enhancement of Quantum Dot−phosphor Hybrid White-light-emitting Diodes Using a Centrifugation-based Quasi-horizontal Separation Structure. *Opt. Express* **2020**, *28*, 13279−13289.

(16) Yu, X.; Shu, W.; Hu, R.; Xie, B.; Ma, Y.; Luo, X. Dynamic Phosphor Sedimentation Effect on the Optical Performance of White LEDs. *IEEE Photonics Technol. Lett.* **2017**, *29*, 1195−1198.
(17) Zhuang, Y.; Wang, Y.; Wang, L.; Li, Z.; Li, W.; Yang, L.; Zou, J. Effect of Phosphor Sedimentation on Photochromic Properties of a Warm White Light-emitting Diode. *J. Semicond.* **2018**, *39*, No. 124006.
(18) Guo, B.; Xu, J.; Liu, S.; Wu, J. N.; et al. Improved Anti-sedimentation for Acrylic Resin Containing Long Afterglow Phosphors by In Situ Polymerization. *Pigm. Resin Technol.* **2012**, *41*, 91−94.
(19) Lei, X.; Zheng, H.; Liu, S.; Luo, X. Performance Enhancement of White LEDs Through Phosphor/Silicone Composite Particles. *IEEE Photonics Technol. Lett.* **2015**, *27*, 1060−1063.
(20) Peng, Y.; Mou, Y.; Zhuo, Y.; Li, H.; Wang, X.; Chen, M.; Luo, X. Preparation and Luminescent Performances of Thermally Stable Red-emitting Phosphor-in-glass for High-power Lighting. *J. Alloys Compd.* **2018**, *768*, 114−121.
(21) Chung, W. J.; Nam, Y. H. Review—A Review on Phosphor in Glass as a High Power LED Color Converter. *ECS J. Solid State Sci. Technol.* **2019**, *9*, No. 016010.
(22) Zhuang, J.; Xia, Z.; Liu, H.; Zhang, Z.; Liao, L. The Improvement of Moisture Resistance and Thermal Stability of $Ca_3SiO_4Cl_2$:Eu^{2+} Phosphor Coated with SiO2. *Appl. Surf. Sci.* **2011**, *257*, 4350−4353.
(23) Yoo, H.; Jang, H. S.; Lee, K.; Woo, K. Quantum dot-layer-encapsulated and Phenyl-functionalized Silica Spheres for Highly Luminous, Colour Rendering, and Stable White Light-emitting Diodes. *Nanoscale* **2015**, *7*, 12860−12867.
(24) Chanyawadee, S.; Lagoudakis, P. G.; Harley, R. T.; Charlton, M. D. B.; Talapin, D. V.; Huang, H. W.; Lin, C.-H. Increased Color-Conversion Efficiency in Hybrid Light-Emitting Diodes utilizing Non-radiative Energy Transfer. *Adv. Mater.* **2010**, *22*, 602−606.
(25) Ghataora, S.; Smith, M. R.; Athanasiou, M.; Wang, T. Electrically Injected Hybrid Organic/inorganic III-nitride White Light-emitting Diodes with Nonradiative Förster Resonance Energy Transfer. *ACS Photonics* **2018**, *5*, 642−647.

https://dx.doi.org/10.1021/acsanm.0c02947
ACS Appl. Nano Mater. 2020, 3, 12394−12400